https://doi.org/10.7840/kics.2023.48.1.23

불완전한 SIC에서 비동축 OAM-NOMA의 용량 해석

카윰 압둘라•, 신 수 용°

Capacity Analysis of Non-Coaxial OAM-NOMA Under Imperfect SIC

Qayyum Abdullah•, Soo Young Shin°

요 약

궤도 각운동량(OAM, Orbital Angular Momentum)은 미래 6G 통신을 위한 후보 기술 중 하나이며, 비직교 다중 접속(NOMA, Non-orthogonal Multiple Access)와 결합하여 데이터 용량을 향상시킬 수 있다. 본 논문에서는 송신부의 고정 전력 할당과 수신부의 다중 사용자 신호 간섭 제거 (SIC, Successive Interference Cancellation)를 고려한다. 현실적인 시나리오에서는 SIC에서 오류가 발생할 수 있기 때문에 이로 인한 SIC 성능 저하가 예상할 수 있다. 본 논문에서는 NOMA 기반 OAM (OAM-NOMA) 시스템에서의 SIC 오류로 인한 영향에 대한 성능 분석을 진행한다. 모의 실험 결과를 보면 OAM-NOMA의 용량은 SIC 오류로 인해 감소하지만 특정 지점을 기준으로 OMA-OAM 혹은 NOMA 시스템보다 성능이 뛰어남이 확인된다.

Key Words : 6G, Wireless communication, Non-orthogonal multiple access (NOMA), Orbital angular momentum (OAM), Imperfect successive interference cancellation (SIC)

ABSTRACT

Orbital angular momentum is one of the best candidates for future 6G communication and in combination with NOMA, enhanced data rates can be achieved by utilizing non-orthogonal resource allocation of NOMA and orthogonal OAM modes. In this paper, at the transmitter side fixed power allocation and at the receiver side, successive interference cancelation (SIC) for the removal of multiuser interference is considered. In practical scenarios, in the SIC process, errors can occur leading to residual interference reducing the system capacity. This paper analyzes the effect of imperfection in successive interference cancellation (SIC) for non-coaxial orbital angular momentum based non-orthogonal multiple access (NOMA) communication for multiple users. The simulation results show that although the capacity of OAM-NOMA reduces with the imperfect SIC but it performs better than the conventional methods such as orthogonal multiple access (OMA-OAM) and NOMA when the error in SIC process is not too large.

※ This work was supported by the National Research Foundation of Korea(NRF) grant funded by the Korea government. (MSIT) (No. 2022R1A2B5B01001994)
※ This research was supported by Basic Science Research Program through the National Research Foundation of Korea(NRF) funded by the Ministry of Education(No. 2022R1I1A1A01069334)
• First Author : Kumoh National Institute of Technology, Dept. of IT Convergence Engineering, khan0253@kumoh.ac.kr, 정회원
° Corresponding Author : Kumoh National Institute of Technology, Dept. of IT Convergence Engineering, wdragon@kumoh.ac.kr, 종신회원
논문번호 : 202211-264-A-RE, Received October 31, 2022; Revised November 15, 2022; Accepted November 15, 2022

Ⅰ. Introduction

The data hungry applications such as virtual reality (VR), augmented reality (AR) and massive internet of things (mIoT) will require a higher data rate as well as reliability which has motivated research towards the next generation of wireless communication which is 6G. 6G is expected to solve these problems as the expected data rate of 6G will be ten times higher than that of 5G with a peak data rate of up to 1THz/sec and reliability of 99.99999%[1]. Different technologies are being explored for the future 6G wireless communication and orbital angular momentum is one of the technologies receiving attention in this regard[2].

Orbital angular momentum (OAM) refers to the wavefront propagating with the spiral phase front and was proven to have applications in wireless communication[3]. OAM provides another degree of freedom (DoF) for data transmission with the help of OAM modes, unlike other conventional technologies where a signal is transmitted using amplitude, phase, time, frequency and/or polarization. These OAM modes are orthogonal to each other when transmitter and receiver are coaxial, hence, there is no inter-symbol interference (ISI) and inter-mode interference (IMI) and multiple OAM modes can be transmitted simultaneously, which greatly improves capacity.

Different methods have been introduced for the generation of OAM using different antenna types such as spiral phase antenna[4], resonant cavity[5], metamaterials[6] and phased antenna arrays[7]. The most common type of antenna for the generation of OAM is a uniform circular array (UCA), which is also used in this paper. Several experiments have been conducted to prove the effectiveness of OAM in wireless communication. The first such experiment was conducted by NTT and NTT successfully transmitted data over 10 meters distance with a data rate of 100 Gbps[8]. OAM can be also utilized for long-distance communication as the validity of OAM for long-distance communication is proved in [9]. OAM is combined with other technologies such as MIMO[10] and NOMA[11] for further enhancement of data rate.

Non-orthogonal multiple access (NOMA) is a multiple access technique in which multiple users are multiplexed together either in the power domain or code domain[12]. In the downlink power domain NOMA, different power is allocated for different users based on their channel conditions and due to low complexity fixed power allocation (FPA) is adopted. In the case of FPA, each user is assigned with a fixed power based on the distance from the base station so the user with the maximum distance from the base station gets high power allocation by the base station as compared to the near users. This power allocation has a significant effect on the overall performance of NOMA. By utilizing this power difference, the users decode their signals. In other words, different users' data is transmitted using a single superimposed signal with the exploitation of the power domain in a single resource block[13]. This resource sharing among the users leads to interference which can be mitigated with the help of successive interference cancelation (SIC) at the receiver side[14].

In the SIC process, the users receive a superimposed signal, decode the information with the higher power allocation and subtract it from the total signal to extract the information with the low power[12]. Moreover, SIC is performed by the users in the order of higher channel gains and the user with the lowest channel gain does not perform SIC. As the number of users increases, the decoding time and the receiver complexity also increase as SIC has to be done several times[15]. Moreover, in practical scenarios errors can occur in the SIC process resulting the deterioration of the capacity.

NOMA-OAM-MIMO is proposed in [16] for the capacity enhancement with perfect SIC and two users' case with misalignments between the base station and users. In [11], authors have explored NOMA-OAM system and compared with OMA-OAM, also the transmitter and receivers are coaxial to each other and perfect SIC is assumed. To the best of authors' knowledge, there is no prior work about the NOMA-OAM for multiple users with imperfect SIC and misaligned case of

transmitter and receiver. So, in this paper, the effect of imperfection in SIC on the performance of OAM-NOMA for multiple users is analyzed while also considering the misalignment issues between the transmitter and receivers. The effect of different power allocation on the sum capacity is also analyzed using simulation results. Moreover, the simulation results show that with the imperfect SIC the system capacity reduces but is still higher than other schemes when the imperfection in SIC is small.

The remaining of the paper is organized as: section II explains the system model, and in section III capacity analysis is discussed. Section IV analyzes the results and finally, the paper is concluded in section V.

Ⅱ. System Model

In this paper, downlink OAM-NOMA with three users is considered as shown in Fig. 1. There is a base station (BS) having a uniform circular array (UCA) with N antenna elements and three users namely near user as U_1, middle user as U_2 and far user as U_3, each user is equipped with a single uniform circular array (UCA) having M antenna elements. These elements in the UCAs are uniformly distributed around the circle. The distance between the centers of UCA at the base station and the center of UCA at U_i is d_i $i\epsilon$ {1,2,3}. Also, the distance between the n^{th} antenna element of the base station UCA and the m^{th} antenna element of receiver UCA at U_i is $d_{i(m,n)}$. Using this configuration, the total available modes are $\Gamma = min(M, N)$. By utilizing Γ $(0 \le l \le \Gamma - 1)$ OAM modes, BS transmits data towards the users with different power allocation within each OAM mode having perfect channel state information (CSI).

For N antenna elements, the transmit data vector is:

$$\boldsymbol{\Omega} = [\Omega_0, \Omega_1, \dots, \Omega_{N-1}] \tag{1}$$

As per the NOMA principle,

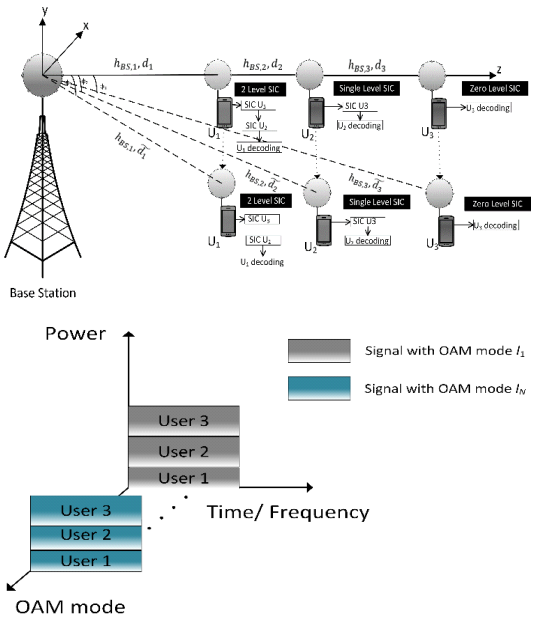

Fig. 1. Non-Coaxial OAM-NOMA system model

$$\Omega = \sqrt{\alpha_1 P}x_1 + \sqrt{\alpha_2 P}x_2 + \sqrt{\alpha_3 P}x_3 \tag{2}$$

where α_1, α_2 and α_3 are the power allocation factors for U_1, U_2 and U_3, P is the total power, and x_1, x_2 and x_3 are the data symbols intended for U_1, U_2 and U_3, respectively. The modulation of Ω_l with the OAM mode l is:

$$\boldsymbol{\xi}_l = \left[\Omega_l e^{\frac{j2\pi}{N}l*0}, \Omega_l e^{\frac{j2\pi}{N}l*1}, \dots, \Omega_l e^{\frac{j2\pi}{N}l*(N-1)}\right] \tag{3}$$

As discussed earlier the total OAM modes are Γ $(0 \le l \le \Gamma - 1)$ For the process of transmitting multiple OAM modes simultaneously, modulation vectors are multiplexed together:

$$\boldsymbol{s} = \sum_{l=0}^{\Gamma-1} \boldsymbol{\xi}_l$$

$$= \sum_{l=0}^{\Gamma-1} \left[\Omega_l e^{\frac{j2\pi}{N}l*0}, \Omega_l e^{\frac{j2\pi}{N}l*1}, \dots, \Omega_l e^{\frac{j2\pi}{N}l*(N-1)}\right] \tag{4}$$

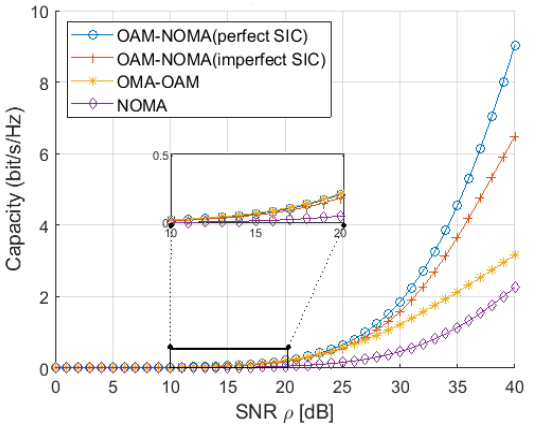

Fig. 2. U_1 capacity vs SNR.

The channel matrix with misalignment of BS and users U_1, U_2 and U_3, between the n^{th} antenna element of the UCA at BS and the m^{th} antenna element of U_i is[16]:

$$\boldsymbol{h}_{i_{(m,n)}} = A_m e^{-j\left[B_m \sin\left(\frac{2\pi(n-1)}{N} - \psi_m + \zeta_m\right)\right]}, \quad (5)$$

where,

$$A_m = \frac{\beta\lambda}{4\pi\sqrt{\left(d_{i_{(m,n)}}^2 + r_n^2 + R_m^2\right)}} e^{\frac{-j2\pi\sqrt{\left(d_{i_{(m,n)}}^2 + r_n^2 + R_m^2\right)}}{\lambda}} \quad (6)$$

and

$$B_m = \frac{2\pi r_n \sqrt{R_m^2 + d_{i_{(m,n)}}^2 \sin^2\phi_i - 2R_m d_{i_{(m,n)}}^2 \sin\phi_i \cos(\psi_m - \theta)}}{\lambda\sqrt{\left(d_{i_{(m,n)}}^2 + r_n^2 + R_m^2\right)}} \quad (7)$$

The basic angle of the m^{th} antenna element at user U_i is $\psi_m = 2\pi(m-1)/M$. The attenuation and phase rotations caused by the antenna elements in denoted by β and has a constant value. R_m and r_n denote the UCA radius at the users and base station. λ is the wavelength of the carrier frequency. θ is the included angle between the x- axis and the projection of the line from the center of the Tx UCAs to the center of receiving UCAs on the transmit plane. ϕ_1, ϕ_2 and ϕ_3 are the included angles between the z-axis and the line connecting the centers of base station UCA and receivers' U_1, U_2 and U_3 UCAs. ζ_m can be defined as:

$$\sin\zeta_m = \frac{R_m - d_{i_{(m,n)}} \sin\phi_i \cos(\psi_m - \theta)}{\sqrt{R_m^2 + d_{i_{(m,n)}}^2 \sin^2\phi_i - 2R_m d_{i_{(m,n)}} \sin\phi_i \cos(\psi_m - \theta)}} \quad (8)$$

and

$$\cos\zeta_m = \frac{d_{i_{(m,n)}} \sin\phi_i \cos(\psi_m - \theta)}{\sqrt{R_m^2 + d_{i_{(m,n)}}^2 \sin^2\phi_i - 2R_m d_{i_{(m,n)}} \sin\phi_i \cos(\psi_m - \theta)}} \quad (9)$$

Where ϕ_i is the angle between the z-axis and the central line from the UCA at the BS to the user U_1.

The OAM signal received by the users U_1, U_2 and U_3 can be represented as

$$y_1 = \sum_{m=1}^{M}\sum_{n=1}^{N} \boldsymbol{s}h_{1_{(m,n)}} e^{j\frac{2\pi(n-1)}{N} l_n} + z_{m_{u_1}}, \quad (10)$$

$$y_2 = \sum_{m=1}^{M}\sum_{n=1}^{N} \boldsymbol{s}h_{2_{(m,n)}} e^{j\frac{2\pi(n-1)}{N} l_n} + z_{m_{u_2}}, \quad (11)$$

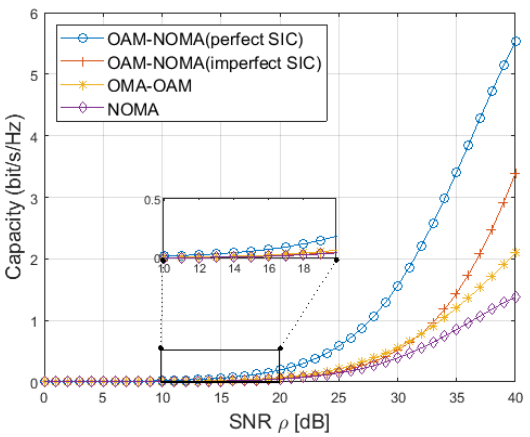

Fig. 3. U_2 capacity vs SNR.

$$y_3 = \sum_{m=1}^{M}\sum_{n=1}^{N} \boldsymbol{s}h_{3_{(m,n)}} e^{j\frac{2\pi(n-1)}{N}l_n} + z_{m_{u_3}}, \quad (12)$$

Where $z_{m_{u_1}}$, $z_{m_{u_2}}$ and $z_{m_{u_3}}$ are the random AWGN with zero mean and variance δ^2 at m^{th} receive antenna element of the user U_1, U_2 and U_3, respectively.

Ⅲ. Capacity Analysis

The signal to noise ratio (SNR) for users U_1, U_2 and U_3, with imperfect SIC is

$$\Upsilon_1 = \sum_{m=1}^{M}\sum_{n=1}^{N} \frac{\rho\left|h_{1_{(m,n)}}\right|^2 \alpha_1}{\kappa\alpha_2\left|h_{1_{(m,n)}}\right|^2 \rho + \kappa\alpha_3\left|h_{1_{(m,n)}}\right|^2 \rho + 1}, \quad (13)$$

$$\Upsilon_2 = \sum_{m=1}^{M}\sum_{n=1}^{N} \frac{\rho\left|h_{2_{(m,n)}}\right|^2 \alpha_2}{\alpha_1\left|h_{2_{(m,n)}}\right|^2 \rho + \kappa\alpha_3\left|h_{2_{(m,n)}}\right|^2 \rho + 1}, \quad (14)$$

$$\Upsilon_3 = \sum_{m=1}^{M}\sum_{n=1}^{N} \frac{\rho\left|h_{3_{(m,n)}}\right|^2 \alpha_3}{\alpha_1\left|h_{3_{(m,n)}}\right|^2 \rho + \alpha_2\left|h_{3_{(m,n)}}\right|^2 \rho + 1}, \quad (15)$$

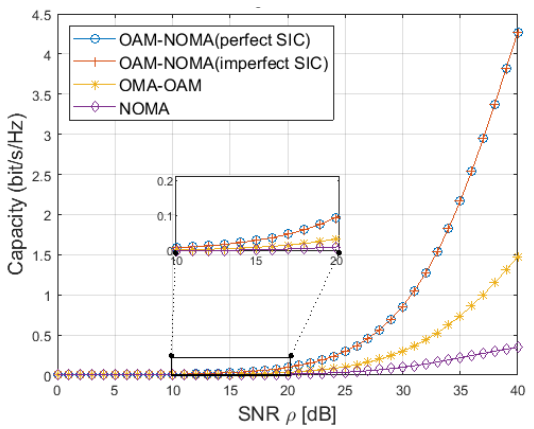

Fig. 4. U_3 capacity vs SNR.

where $\rho = \frac{P}{\delta^2}$ is transmit SNR and $\kappa \in [0,1]$ is the SIC imperfection parameter which arises when the receiver is unable to remove the interference caused by other users' signals[18].

The capacity equations for U_1, U_2, U_3 and sum capacity denoted as C_{u_1}, C_{u_2}, C_{u_3} and C_s, respectively, can be expressed as

$$C_{u_1} = \sum_{q_1=1}^{Q_1} \log_2\left(1 + \frac{\Upsilon_1}{N}\varrho_{q_1}^2\right), \quad (16)$$

$$C_{u_2} = \sum_{q_2=1}^{Q_2} \log_2\left(1 + \frac{\Upsilon_2}{N}\varrho_{q_2}^2\right), \quad (17)$$

$$C_{u_3} = \sum_{q_3=1}^{Q_3} \log_2\left(1 + \frac{\Upsilon_3}{N}\varrho_{q_3}^2\right), \quad (18)$$

$$C_s = C_{u_1} + C_{u_2} + C_{u_3} \quad (19)$$

where $\varrho_{q_1}^2$, $\varrho_{q_2}^2$ and $\varrho_{q_3}^2$ are the channel eigenvalues for U_1, U_2 and U_3, respectively. Furthermore, $Q_i \leq R_i = \min(M, N)$ and full rank matrices which are $Q_i = R_i$ are considered in this paper.

For OMA-OAM, the rate equations for U_1, U_2 and U_3 and sum capacity denoted as $C_{u_1}^{OMA}$, $C_{u_2}^{OMA}$, $C_{u_3}^{OMA}$ and C_{sum}^{OMA}, respectively, can be expressed as

$$C_{u_1}^{OMA} = \sum_{q_1=1}^{Q_1} \frac{1}{3}\log_2\left(1 + \Upsilon_{u_1}^{OMA}\varrho_{q_1}^2\right), \quad (20)$$

$$C_{u_2}^{OMA} = \sum_{q_2=1}^{Q_2} \frac{1}{3}\log_2\left(1 + \Upsilon_{u_2}^{OMA}\varrho_{q_2}^2\right), \quad (21)$$

$$C_{u_3}^{OMA} = \sum_{q_3=1}^{Q_3} \frac{1}{3}\log_2\left(1 + \Upsilon_{u_3}^{OMA}\varrho_{q_3}^2\right), \quad (22)$$

$$C_{sum}^{OMA} = C_{u_1}^{OMA} + C_{u_2}^{OMA} + C_{u_3}^{OMA} \quad (23)$$

where

$$\Upsilon_1^{OMA} = \sum_{m=1}^{M}\sum_{n=1}^{N} \rho\left|h_{1_{(m,n)}}\right|^2 P, \quad (24)$$

$$\Upsilon_2^{OMA} = \sum_{m=1}^{M}\sum_{n=1}^{N} \rho \left|h_{2_{(m,n)}}\right|^2 P, \quad (25)$$

$$\Upsilon_3^{OMA} = \sum_{m=1}^{M}\sum_{n=1}^{N} \rho \left|h_{3_{(m,n)}}\right|^2 P, \quad (26)$$

The factor $\frac{1}{3}$ is the eq. (20-22) indicate that there is a multiplexing loss of $\frac{1}{3}$ due to the division in a resource block that is time in this case because time division multiple access (TDMA) is utilized to serve the users.

In case of NOMA, the capacity equations can be given as:

$$C_{u_1}^{NOMA} = \log_2\left(1 + \frac{\rho|h_1|^2\alpha_1}{\kappa\alpha_2|h_1|^2\rho + \kappa\alpha_3|h_1|^2\rho + 1}\right), \quad (27)$$

$$C_{u_2}^{NOMA} = \log_2\left(1 + \frac{\rho|h_2|^2\alpha_2}{\alpha_1|h_2|^2\rho + \kappa\alpha_3|h_2|^2\rho + 1}\right), \quad (28)$$

$$C_{u_3}^{NOMA} = \log_2\left(1 + \frac{\rho|h_3|^2\alpha_3}{\alpha_1|h_3|^2\rho + \alpha_2|h_3|^2\rho + 1}\right), \quad (29)$$

$$C_{sum}^{NOMA} = C_{u_1}^{NOMA} + C_{u_2}^{NOMA} + C_{u_3}^{NOMA} \quad (30)$$

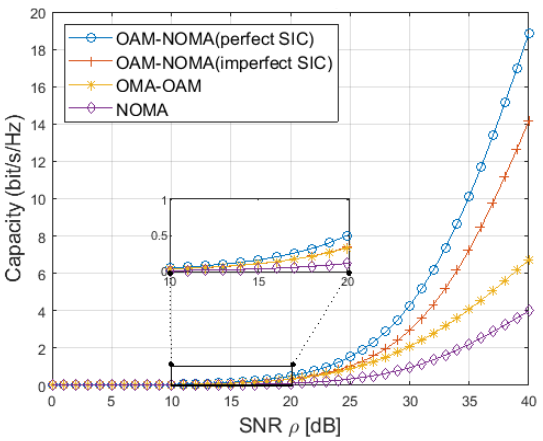

Fig. 5. Sum capacity vs SNR.

Ⅳ. Result Analysis

In this section, the simulation results which show the effect of imperfect SIC on the capacity of OAM-NOMA are presented for three user case. The simulation parameters are $M = N = 4$, $\alpha_1 = 0.05$, $\alpha_2 = 0.15$, $\alpha_3 = 0.8$ fixed power allocation is adopted[19], $\beta = 4\pi$, λ =0.01m, $R_m = r_n = \lambda$, $d_1 = 10\lambda$, $d_2 = 20\lambda$, $d_2 = 30\lambda$ $\phi_1 = \phi_2 = \phi_3 = \theta = 0$, κ = 0.01 and $P = 1$. As you can see in Fig. 2-5, OAM-NOMA provides better results than the other schemes that are OMA-OAM and NOMA and it is because of the OAM, multiple orthogonal beams serve the users in the same resource block(time/frequency) which is only used to serve a single user in case of OMA-OAM resulting in low capacity for OMA-OAM. The capacity values for NOMA are the lowest as in one resource block one beam is serving both users. In the case of perfect SIC, the capacity increases linearly but when there is an imperfection in the SIC process, the near user U_1, and middle user U_2, capacity increases up to a certain point and then approaches a constant value capacity increases up to a certain point and then approaches a constant value and is always less than the perfect SIC case as in Fig. 1. In Fig. 4, it can be seen that the capacity for both perfect SIC and imperfect SIC cases remains the same which is due to the fact that in NOMA, far user do not perform SIC.

In Fig. 6, sum capacity of the system is analyzed by allocating different powers to different users. It is clear from Fig. 6 that this system is more robust to the changes in the power allocations. As by increasing or decreasing power allocation of a user, its capacity increased or decreased, respectively, but the overall, system performance nearly remains the same.

In Fig. 7, sum capacity is analyzed for different values of imperfect SIC parameter ($\kappa = 0.01$, $\kappa = 0.05$ and $\kappa = 0.1$) and perfect SIC ($\kappa = 0$) and it is obvious that if the imperfection in SIC is increased significantly, OAM-NOMA performance deteriorates in such a way that its capacity reduces significantly which shows that the large errors in

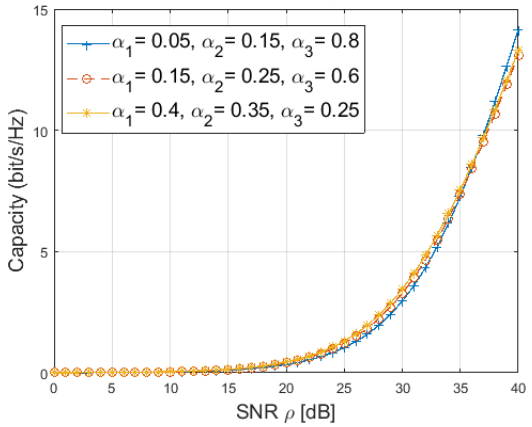

Fig. 6. Sum capacity vs SNR for different power allocations.

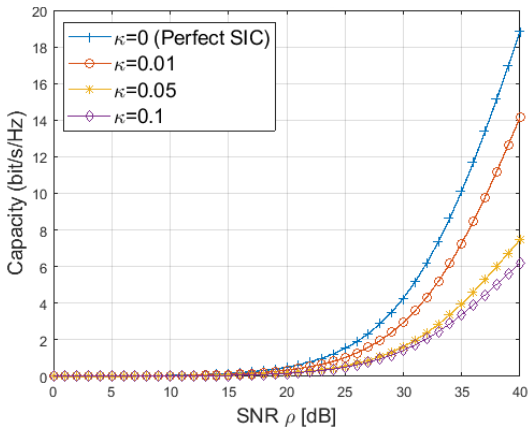

Fig. 7. Sum capacity vs SNR for different values of imperfect SIC parameter.

SIC can significantly reduce the OAM-NOMA system capacity.

V. Conclusion

In this paper, the capacity of OAM-NOMA is analyzed with imperfect SIC for three users. It has been proved using simulation results that the OAM-NOMA system with imperfect SIC provides better capacity as compared with other conventional schemes when the error in SIC is not too large. In future, this system can be analyzed with imperfect channel state information as well as OAM inter-mode interference and OAM mode divergence issues. Furthermore, this system can be analyzed with deep learning and for uplink transmission [20, 21].

References

[1] G. Gui, M. Liu, F. Tang, N. Kato, and F. Adachi, “6G: Opening new horizons for integration of comfort, security, and intelligence,” in *IEEE Wireless Commun.*, vol. 27, no. 5, pp. 126-132, Oct. 2020. (https://doi.org/10.1109/MWC.001.1900516)

[2] C. Yizhan, W. Zhong, H. Da, and L. Ruosen, “6G Is Coming: Discussion on key candidate technologies and application scenarios,” *2020 Int. Conf. CCNS*, pp. 59-62, 2020. (https://doi.org/10.1109/CCNS50731.2020.00022)

[3] B. Thidé, H. Then, J. Sjöholm, K. Palmer, J. Bergman, T. D. Carozzi, Ya. N. Istomin, N. H. Ibragimov, and R. Khamitova, “Utilization of photon orbital angular momentum in the low-frequency radio domain,” in *Phys. Rev. Lett.*, vol. 99, no. 8, Aug. 2007. (https://doi.org/10.1103/PhysRevLett.99.087701)

[4] F. E. Mahmouli and S. D. Walker, “4-Gbps uncompressed video transmission over a 60-GHz orbital angular momentum wireless channel,” in *IEEE Wireless Commun. Lett.*, vol. 2, no. 2, pp. 223-226, Apr. 2013. (https://doi.org/10.1109/WCL.2013.012513.120686)

[5] Y. Pan, et al., “Generation of orbital angular momentum radio waves based on dielectric resonator antenna,” in *IEEE Ant. and Wireless Propag. Lett.*, vol. 16, pp. 385-388, 2017. (https://doi.org/10.1109/LAWP.2016.2578958)

[6] K. Guo, Q. Zheng, Z. Yin, and Z. Guo, “Generation of mode-reconfigurable and frequency-adjustable OAM beams using dynamic reflective metasurface,” in *IEEE Access*, vol. 8, pp. 75523-75529, 2020. (https://doi.org/10.1109/ACCESS.2020.2988914)

[7] D. Lee, H. Sasaki, H. Fukumoto, Y. Yagi, and T. Shimizu, “An evaluation of orbital angular momentum multiplexing technology,” in *Applied Sci.*, vol. 9, no. 9, 2019.

(https://doi.org/10.3390/app9091729)

[8] H. Fukumoto, H. Sasaki, D. Lee, and T. Nakagawa, "Beam divergence reduction using dielectric lens for orbital angular momentum wireless communications," *2016 ISAP*, pp. 680-681, 2016.

[9] Y. Yao, X. Liang, W. Zhu, J. Geng, and R. Jin, "Experiments of orbital angular momentum phase properties for long-distance transmission," in *IEEE Access*, vol. 7, pp. 62689-62694, 2019. (https://doi.org/10.1109/ACCESS.2019.2916029)

[10] K. A. Opare, Y. Kuang, and J. J. Kponyo, "Mode combination in an ideal wireless OAM-MIMO multiplexing system," in *IEEE Wireless Commun. Lett.*, vol. 4, no. 4, pp. 449-452, Aug. 2015. (https://doi.org/10.1109/LWC.2015.2434375)

[11] M. Jian, Y. Chen, and G. Yu, "Improving multiple-user capacity through downlink NOMA in OAM systems," *2021 IEEE ICC Wkshps.*, pp. 1-6, 2021. (https://doi.org/10.1109/ICCWorkshops50388.2021.9473665)

[12] S. M. R. Islam, N. Avazov, O. A. Dobre, and K.-S. Kwak, "Power-domain non-orthogonal multiple access (NOMA) in 5G systems: Potentials and challenges," in *IEEE Commun. Surv. & Tuts.*, vol. 19, no. 2, pp. 721-742, Secondquarter 2017. (https://doi.org/10.1109/COMST.2016.2621116)

[13] T. Manglayev, R. C. Kizilirmak, Y. H. Kho, N. Bazhayev, and I. Lebedev, "NOMA with imperfect SIC implementation," *IEEE EUROCON 2017 - 17th Int. Conf. Smart Technol.*, pp. 22-25, 2017. (https://doi.org/10.1109/EUROCON.2017.8011071)

[14] A. Li, Y. Lan, X. Chen, and H. Jiang, "Non-orthogonal multiple access (NOMA) for future downlink radio access of 5G," in *China Commun.*, vol. 12, no. Supplement, pp. 28-37, Dec. 2015. (https://doi.org/10.1109/CC.2015.7386168)

[15] S. Verdu, "*Multiuser Detection*," Cambridge University Press, Cambirdge, 1998.

[16] A. A. Amin and S. Y. Shin, "Channel capacity analysis of non-orthogonal multiple access with OAM-MIMO system," in *IEEE Wireless Commun. Lett.*, vol. 9, no. 9, pp. 1481-1485, Sep. 2020. (https://doi.org/10.1109/LWC.2020.2994355)

[17] W. Saetan and S. Thipchaksurat, "Power allocation for sum rate maximization in 5G NOMA system with imperfect SIC: A deep learning approach," *2019 4th InCIT*, pp. 195-198, 2019. (https://doi.org/10.1109/INCIT.2019.8911864)

[18] S. Mouni, A. Kumar, and P. K. Upadhyay, "Adaptive user pairing for NOMA systems with imperfect SIC," in *IEEE Wireless Commun. Lett.*, vol. 10, no. 7, pp. 1547-1551, Jul. 2021. (https://doi.org/10.1109/LWC.2021.3074036)

[19] N. Rahayu and Iskandar, "Multiple user fairness power allocation for downlink NOMA," *2021 7th ICWT*, pp. 1-5, 2021. (https://doi.org/10.1109/ICWT52862.2021.9678478)

[20] M. Ahmad, I N. A. Ramatryana, and S.Y. Shin, "Deep learning Enabled MIMO-NOMA System: A Genesis of 6G and Artificial Intelligence", in *Proc. KICS Winter Conference (KICS 2021), pp 259-262, Jeju Island, Korea, February 2021*

[21] I. Azam, and S.Y. Shin, "User Pairing and Power allocation Technique for Uplink NOMA", in *Proc. KICS Summer Conference (KICS 2019), pp 1531-1532, Jeju Island, Korea, June 2019.*

카윰 압둘라 (Qayyum Abdullah)

2019년 8월 : University of Engineering and Technology, Peshawar, Department of Electrical Engineering, B.S

<관심분야> B5G/6G 무선 접속기술, OAM, NOMA

[ORCID:0000-0002-0132-1039]

신 수 용 (Soo Young Shin)

1999년 2월 : 서울대학교 전기공학부 졸업

2001년 2월 : 서울대학교 전기공학부 석사

2006년 2월 : 서울대학교 전기공학부 박사

2010년~현재 : 금오공과대학교 전자공학부 교수

<관심분야> 차세대 무선통신 기술, 드론 응용, 블록체인, 머신러닝, 딥러닝, 혼합현실

[ORCID:0000-0002-2526-2395]